



## Divergent channel flow of Casson fluid and heat transfer with suction/blowing and viscous dissipation: Existence of boundary layer

Astick Banerjee<sup>a</sup>, Sanat Kumar Mahato<sup>a</sup>, Krishnendu Bhattacharyya<sup>b,\*</sup>, Ali J. Chamkha<sup>c</sup>

<sup>a</sup> Department of Mathematics, Sidho-Kanho-Birsha University, Purulia 723104, West Bengal, India

<sup>b</sup> Department of Mathematics, Institute of Science, Banaras Hindu University, Varanasi 221005, Uttar Pradesh, India

<sup>c</sup> Faculty of Engineering, Kuwait College of Science and Technology, Doha District, Kuwait

### ARTICLE INFO

#### Keywords:

Divergent channel  
Casson fluid  
Existence of boundary layer  
Suction/blowing  
Viscous dissipation

### ABSTRACT

The boundary layer existence in divergent porous channel of non-Newtonian Casson fluid with heat transfer in presence of suction/blowing and viscous dissipation is studied. Nonlinear coupled ODEs are obtained from governing PDEs and the conditions under which boundary layer structure for Casson fluid exists by controlling backflow are explored. Numerical solutions are also obtained using “bvp4c”, a MATLAB package. The study reveals that if mass suction exceeds a certain amount which is dependent on Casson parameter then only boundary layer flow is possible and as Casson parameter increases, the requirement of mass suction for boundary layer flow reduces. In addition, rheological characters of Casson fluid and viscous dissipation have a major impact on temperature distribution and due to these, the temperature falls lower than free stream temperature within the boundary layer region.

### 1. Background of the problem

Boundary layer flows in convergent channels and in divergent channels are completely different in the existence point of view. The former one can normally exist, but the latter one is not usually found and with backflow region boundary layer separation occurs depending on the Reynolds number. So, the structure of boundary layer in close neighbourhood of both channel walls will be a possibility if something else can stop the backflow construction, i.e., the cause of separation. In this regard, the pioneering works on converging channels and diverging channels were discussed by Jeffery<sup>1</sup> and Hamel<sup>2</sup> and in their study channel walls are assumed to be motionless and the flow occurs due to presence of a fluid mass sink/source in joining of two channel walls. Pohlhausen<sup>3</sup> described an analytical solution of flow in boundary layer inside a convergent channel. The stability analysis for divergent flow under small disturbance was discussed by Dean<sup>4</sup>. Fraenkel<sup>5,6</sup> reported a certain set of Jeffery–Hamel profiles, in the form of exact solutions. The creeping motion for Newtonian fluid in converging channel disregarding the transverse pressure gradient was discussed by Wang and Price<sup>7</sup>. Ghoneim<sup>8</sup> spoke about converging unidirectional flow of Generalized Newtonian fluids (GNF). Bariş<sup>9</sup> demonstrated steady converging flow of second-grade non-Newtonian fluid. Magyari<sup>10</sup> illustrated convergent channel flow using Pohlhausen<sup>3</sup> solution taking channel wall temperature in power-law variation. Yousefi-Lafouraki et al.<sup>11</sup> reported the entropy generation for shear-thinning nanofluid flow in converging channel and they concluded that the entropy generation for Newtonian

nanofluid is less than non-Newtonian nanofluid. Maranzoni et al.<sup>12</sup> discussed side weir converging flow by both experimental and numerical means.

It is well-known that the introduction of mass suction/blowing in a flow field can change the whole dynamics of flow and also complete heat transfer procedure because it has the capacity to affect the mainstream flow. In addition, suction/blowing has an enormous impact on many engineering activities, especially, on those which involve channel flow or heat transfer. Now, the belief that at high Reynolds numbers, divergent diffuser flow cannot be separated into an inviscid mainstream and thin boundary layer on two walls like the convergent flow, is not correct. In this consequence, Holstein<sup>13</sup> explained that if a considerable amount of mass suction of fluid is applied through porous channel of diverging flow with a high Reynolds number then it will show boundary layer structure. The heat transfer for this flow was illustrated by Gersten and Körner.<sup>14</sup> Eagles<sup>15</sup> argued on the stability of various Jeffery–Hamel solutions for divergent channel flow and Kamel<sup>16</sup> examined the similar steady diverging flow of micropolar fluid. Dennis et al.<sup>17</sup> described diverging flow in between two walls with imposed inlet and outlet conditions. Whereas, the instability flow through a diverging channel was described by Drazin<sup>18</sup> with the help of bifurcation theory. Sadeghy et al.<sup>19</sup> theoretically examined the impact of external magnetic field in controlling separation of flow in Jeffrey–Hamel viscoelastic flows. Akulenko and Kumakshev<sup>20</sup> explained the multimode viscous flows in diverging channels using the bifurcation phenomenon. Esmaeilpour and

\* Corresponding author.

E-mail address: [krish.math@yahoo.com](mailto:krish.math@yahoo.com) (K. Bhattacharyya).

Ganji<sup>21</sup> found solution of Jeffery–Hamel flow between two solid plane walls having angle  $2\alpha$  using optimal homotopy asymptotic method. Haines et al.<sup>22</sup> explored the significance of similarity solution to practical problem related to the flow in divergent channel. Bhattacharyya and Layek<sup>23</sup> analysed the existence of magnetohydrodynamic(MHD) flow in boundary layer of non-Newtonian dilatant fluid in diverging channel in presence of suction/blowing. Sheikholeslami et al.<sup>24</sup> described analytical solution of MHD Jeffery–Hamel flow of an electrically conducting fluid and nanoparticles using Adomian decomposition method(ADM) and determined that due to presence of nanoparticle boundary layer thickness becomes thicker. Layeket al.<sup>25</sup> derived the steady state-case of MHD flow in diverging porous channel and they established that MHD flow is possible with any suction and even for blowing with suitable choice of magnetic field. Later, several more vital features of divergent/convergent flows in channels were obtained by several scientists.<sup>26–33</sup>

Due to applications of non-Newtonian fluids in several industrial and technological processes, the study of different fluid flow problems taking non-Newtonian fluids grabs attention of several researchers.<sup>34–46</sup> In this context, Casson fluid is a realistic non-Newtonian fluid, which obeys rheological data better than others. To have flow of Casson fluid, the shear stress should exceed a critical value called yield stress. It is worthnoting that our blood is often regarded as Casson fluid. The constitutive equation of Casson fluid was introduced by Casson<sup>47</sup> while describing flow equation of pigment-oil suspensions. Fredrickson<sup>48</sup> stated behaviour of steady-flow of Casson fluid inside tube. Later, Boyd et al.<sup>49</sup> reported oscillatory blood flow considering blood as Casson fluid. Mustafa et al.<sup>50</sup> obtained solution of unsteady boundary layer flow of Casson fluid on moving plate using homotopy analysis method (HAM). The exact solution for Casson fluid flow due to stretching/shrinking sheet was stated by Bhattacharyya et al.<sup>51,52</sup> with and without magnetic effect. Gangadhar et al.<sup>53</sup> discussed 3D Casson fluid flow in porous medium. Several exciting investigations Casson fluid and other Newtonian, as well as non-Newtonian fluids, were available in literature.<sup>54–67</sup>

Due to the importance and impact of suction/blowing on boundary layer existence for various types of fluids flowing in a divergent channel by stopping backflow, i.e., separation of boundary layer, here we are motivated towards the investigation of boundary layer non-Newtonian Casson fluid flow with heat transfer in divergent channel considering suction/blowing and viscous dissipation. This divergent flow problem of Casson fluid is a novel and original investigation if we are able to find existence condition of boundary layer avoiding separation. In due course, transformed ordinary differential equations (ODEs) are obtained and the existence condition of boundary layer structure by controlling back-flow is established. Also, the ODEs are solved numerically and to recognize the impacts of physical involved parameters on flow properties and heat transfer those computed results are presented in graphical mode. It is noteworthy that the considered problem can be applied in flows of blood vessels, river flows, etc. directly or a fairly similar flow occurs there.

## 2. Flow formulation

Consider steady 2D flow of a Casson fluid in divergent channel. The channel walls assume to be stationary and porous, through which mass suction/blowing is imposed. Here, flow near only one channel wall of the channel is described, because identical flow structure should be on the other channel wall. Along the considered wall  $x$ -axis is taken and  $y$ -axis is orthogonal to  $x$ -axis with intersection of two channel walls being the origin. The rheological equation for the flow of isotropic and incompressible Casson fluid may be considered as<sup>54</sup>:

$$\tau_{ij} = \begin{cases} (\mu_B + p_y/\sqrt{2\pi})2e_{ij}, & \pi > \pi_c \\ (\mu_B + p_y/\sqrt{2\pi_c})2e_{ij}, & \pi < \pi_c, \end{cases} \quad (2.1)$$

where  $\mu_B$  is plastic dynamic viscosity of non-Newtonian fluid,  $p_y$  and  $\pi$  are yield stress of fluid and product of deformation-rate component with itself, namely,  $\pi = e_{ij}e_{ij}$ ,  $e_{ij}$  being  $(i, j)$ th deformation rate component and  $\pi_c$  is critical value of above product dependent on non-Newtonian fluid model.

Under aforesaid conditions, steady-state boundary layer equations for Casson fluid flow through a divergent channel are

$$\frac{\partial \bar{u}}{\partial x} + \frac{\partial \bar{v}}{\partial y} = 0, \quad (2.2)$$

$$\bar{u} \frac{\partial \bar{u}}{\partial x} + \bar{v} \frac{\partial \bar{u}}{\partial y} = -\frac{1}{\rho} \frac{\partial \bar{p}}{\partial x} + \nu(1 + 1/\beta) \frac{\partial^2 \bar{u}}{\partial y^2}, \quad (2.3)$$

$$0 = -\frac{1}{\rho} \frac{\partial \bar{p}}{\partial y}, \quad (2.4)$$

where  $\bar{u}$  and  $\bar{v}$  are velocity components in  $x$ - and  $y$ -directions, respectively,  $\nu$  and  $\rho$  are kinematic fluid viscosity and density,  $\beta(= \mu_B \sqrt{2\pi_c}/p_y)$  is Casson parameter. After order analysis of above two momentum equations, it is quite evident that  $|\partial \bar{p}/\partial y| \ll |\partial \bar{p}/\partial x|$ . So, it may be stated that for boundary layer, the pressure  $\bar{p}$  is function of  $x$  only to its first approximation. The full derivation of boundary layer equation for Casson fluid flow from its rheological equation might be found in the article by Bhattacharyya et al.<sup>52</sup>

For velocity components, boundary conditions are

$$\left. \begin{aligned} \bar{u} = 0, \bar{v} = -v_w(x) \text{ at } y = 0 \\ \bar{u} \rightarrow U(x) \text{ for } x > 0 \text{ as } y \rightarrow \infty. \end{aligned} \right\} \quad (2.5)$$

The variable velocity of free-stream is specified as:

$$U(x) = \frac{Q}{\alpha x} = \frac{U_0 L}{x} \quad (U_0 > 0), \quad (2.6)$$

where  $\alpha$  is the angle between the channels,  $Q(>0)$  is a constant,  $U_0$  and  $L$  are characteristic velocity and length, respectively (with  $Q/\alpha = U_0 L$ ).

The velocity of applied suction/blowing,  $v_w(x)$  through porous walls of the divergent channel is given by:

$$v_w(x) = \frac{S\sqrt{Qv}}{x\sqrt{\alpha}}, \quad (2.7)$$

where  $S$  is mass suction/blowing parameter ( $S>0$  and  $S<0$  correspond mass suction and mass blowing). A sketch of flow region of divergent channel and other details are given in Fig. 1.

Since  $\bar{p} = \bar{p}(x)$ , pressure gradient  $\partial \bar{p}/\partial x$  may be derived from (2.3) using free-stream region as:

$$-\frac{1}{\rho} \frac{\partial \bar{p}}{\partial x} = U \frac{dU}{dx}. \quad (2.8)$$

Removing  $\partial \bar{p}/\partial x$  from Eqs. (2.3) and (2.8), we get

$$\bar{u} \frac{\partial \bar{u}}{\partial x} + \bar{v} \frac{\partial \bar{u}}{\partial y} = U \frac{dU}{dx} + \nu(1 + 1/\beta) \frac{\partial^2 \bar{u}}{\partial y^2}. \quad (2.9)$$

The Eqs. (2.2) and (2.9) admit following similarity solution identified as:

$$\bar{u} = \frac{Q}{\alpha x} f(\eta) \text{ and } \bar{v} = \sqrt{\frac{Qv}{\alpha}} [\eta f(\eta) - S]/x, \quad (2.10)$$

where  $\eta$  is the similarity variable and it is defined by  $\eta = (y/x)\sqrt{Q/\alpha\nu}$ .

The continuity equation (2.2) is automatically satisfied and Eq. (2.9) converts to following self-similar equation:

$$(1 + 1/\beta)f'' - (1 - f^2) + Sf' = 0, \quad (2.11)$$

with

$$f(0) = 0, \quad f(\infty) = 1. \quad (2.12)$$

## 3. Possibility of boundary layer flow and separation control

The boundary layer steady-state Casson fluid flow through a divergent channel cannot be possible because of the occurrence of back-flow which results in flow separation. So, conditions under which the

backflow may be prevented and boundary layer separation can be controlled, are really important. Inside the flow region of boundary layer, quantity  $f'(\eta)$ [=  $Z$ , say] is proportional directly to velocity gradient ( $\partial u/\partial y$ ). Now, across boundary layer the quantity  $\partial u/\partial y$  slowly declines and diminishes to zero at border point of boundary layer, this immediately tells that  $Z$  is a monotonically decreasing function of  $\eta$ ; hence  $Z'(\eta) < 0$  inside boundary layer and  $Z \rightarrow 0$  as  $\eta \rightarrow \infty$ . So, as  $\eta$  changes from 0 (at channel wall) to  $\infty$  (in free-stream),  $f(\eta)$  grows from 0 (at channel wall) to 1 (at border-point of boundary layer) thus  $f'(\eta) > 0$ . Therefore,  $dZ/df = (dZ/d\eta)/(df/d\eta)$  is of negative value inside whole boundary layer region and  $Z \rightarrow 0$  as  $f \rightarrow 1$ .<sup>23</sup>

By substituting  $f'(\eta) = Z(dZ/df)$ , self-similar equation (11) is written as:

$$\frac{dZ}{df} = \frac{(1 - f^2) - SZ}{(1 + 1/\beta)Z}. \tag{3.1}$$

Taking limit as  $f \rightarrow 1$  and also  $Z \rightarrow 0$  as  $f \rightarrow 1$ , Eq. (3.1) reduces to

$$\lim_{f \rightarrow 1} \frac{dZ}{df} = \lim_{f \rightarrow 1} \frac{(1 - f^2) - SZ}{(1 + 1/\beta)Z}.$$

In the limit in R.H.S.(right hand side) is in indeterminate form, so it may reduces to

$$\begin{aligned} \lim_{f \rightarrow 1} \frac{dZ}{df} &= \lim_{f \rightarrow 1} \frac{-2f - S \frac{dZ}{df}}{(1 + 1/\beta) \frac{dZ}{df}} \\ \Rightarrow \lim_{f \rightarrow 1} \frac{dZ}{df} &= \frac{-2 - S \lim_{f \rightarrow 1} \frac{dZ}{df}}{(1 + 1/\beta) \lim_{f \rightarrow 1} \frac{dZ}{df}}. \end{aligned}$$

Denoting  $(dZ/df)_{f \rightarrow 1} = \Gamma$ , we can write

$$(1 + 1/\beta)\Gamma^2 + S\Gamma + 2 = 0, \tag{3.2}$$

which provides the two values of  $\Gamma$  as:

$$\Gamma = \frac{1}{2} \left\{ -S \pm \sqrt{S^2 - 8(1 + 1/\beta)} \right\}. \tag{3.3}$$

For existence of boundary layer structure near two channel walls, it should be necessary that value of  $\Gamma$  is negative across the whole boundary layer. So, it is quite clear that if the parameter  $S \geq 2\sqrt{2}\sqrt{1 + 1/\beta}$ , then one of the two values of  $\Gamma$  is negative. Hence for Casson fluid flow in divergent channel boundary layer exists and separation is controlled by preventing backflow only when there is mass suction exceeding a fixed value. Obviously, there is no boundary layer structure for mass blowing case and without mass suction/blowing case when any specific Casson fluid (fixed value of  $\beta$ ) is considered. It is worth noting that as  $\beta \rightarrow \infty$ , Casson fluid is changed to Newtonian fluid and in that case boundary layer flow occurs only when  $S \geq 2\sqrt{2}$ , which is exactly same as described by Holstein.<sup>13</sup>

**4. Heat transfer**

The energy equation for the above described flow with viscous dissipation effect may be presented as:

$$\bar{u} \frac{\partial \bar{T}}{\partial x} + \bar{v} \frac{\partial \bar{T}}{\partial y} = \frac{\kappa}{\rho c_p} \frac{\partial^2 \bar{T}}{\partial y^2} + \frac{v}{c_p} (1 + 1/\beta) \left( \frac{\partial \bar{u}}{\partial y} \right)^2, \tag{4.1}$$

where  $\bar{T}$ ,  $\kappa$  and  $c_p$  are fluid temperature, fluid thermal conductivity and specific heat, respectively.

Boundary conditions are

$$\bar{T} = T_w \text{ at } y = 0; \bar{T} \rightarrow T_\infty \text{ as } y \rightarrow \infty, \tag{4.2}$$

where  $T_w$  and  $T_\infty$  are fixed temperatures along channel wall and at free-stream.

The dimensionless temperature,  $\theta$  is presented as:

$$\bar{T} = T_\infty + (T_w - T_\infty)\theta(\eta). \tag{4.3}$$

Using relations in (2.10) and (4.3), Eq. (4.1) turns into

$$\theta'' + \text{Pr}[S\theta' - Ec(1 + 1/\beta)f'^2] = 0, \tag{4.4}$$

where  $\text{Pr} = \nu\rho c_p/\kappa$  is well-known Prandtl number and  $Ec = U^2/[c_p(T_w - T_\infty)]$  is Eckert number.

Boundary conditions (4.2) become

$$\theta(0) = 1, \theta(\infty) = 0. \tag{4.5}$$

**5. Numerical solution**

To get solutions of coupled non-linear 2nd order differential equations (2.11) and (4.4) with (2.12) and (4.5), MATLAB programme “bvp4c” is used. To solve by “bvp4c”, above two equations are converted into of a first-order system as:

$$f' = g, g' = [(1 - f^2) - Sp]/(1 + 1/\beta); \tag{5.1}$$

$$\theta' = \phi, \phi = \text{Pr}[Ec(1 + 1/\beta)g^2 - S\phi], \tag{5.2}$$

with

$$f(0) = 0 \text{ and } \theta(0) = 1. \tag{5.3}$$

Bvp4c scheme is based on finite-difference method having fourth-order accuracy. Here the tolerance level is taken as  $10^{-5}$ . Suitable guess values for other two initial conditions are assumed to start computation process.

Also, to judge the accurateness of the aforementioned MATLAB scheme, we have re-solved the above Eqs. (5.1) and (5.2) with (5.3) and suitable guess of unknown initial conditions with standard and well-recognized shooting method with RK-4 scheme. Those two sets of computational results are almost identical and the fact can be visualized in Fig. 2, which represents a specific velocity profile ( $\beta = 0.5$  and  $S = 5$ ) obtained by two schemes.

**6. Velocity and temperature variations**

Computed results using “bvp4c” are exhibited graphically in some figures for suitable involved parametric values.

The Casson parameter ( $\beta$ ) impact upon dimensionless velocity profiles and temperature profiles are portrayed in Figs. 3 and 4. For rise of  $\beta$ , velocity gets elevated and corresponding boundary layer thickness (BLT) reduces. Actually, it occurs due to the plasticity of Casson fluid and as  $\beta$  reduces the plasticity of fluid gets amplified, i.e., the yield stress  $p_y$  enlarges, which originates the augmentation of momentum boundary layer thickness. It means if the fluid changed to Casson fluid from Newtonian fluid ( $\beta = \infty$ ) then boundary layer thickness is larger. Similar effect is detected in temperature field in Fig. 4, i.e., the temperature rise is found and physically, with less plasticity convection heat transfer becomes dominant. In Fig. 4, an interesting character is witnessed. Dimensionless temperature goes below zero level inside boundary layer for Casson fluids and this feature is more prominent with smaller  $\beta$ . This happens because of higher plasticity of fluid with decreasing  $\beta$ .

Fig. 5 slows impact of external suction/blowing ( $S$ ) on velocity and it reveals that for stronger mass suction ( $S > 0$ ), fluid velocity enhances and corresponding BLT reduces. Sucking of fluid mass through porous channel wall eases down the possibility of backflow and it also causes the diminution of the momentum BLT. Due to mass suction, fluid layers with higher velocity drive nearer to channel walls and stream velocity is achieved earlier; which causes boundary layer thickness reduction. Whereas, effect of mass suction on temperature (Fig. 6) are different near channel walls and away from the walls. Temperature initially decreases and for large  $\eta$  it slightly increases. Due to mass suction, the fluid with low temperature comes closer to the wall and it causes the decline of temperature near channel walls. Mass suction eases out the influence of Casson parameter in dragging the dimensionless temperature below zero level.

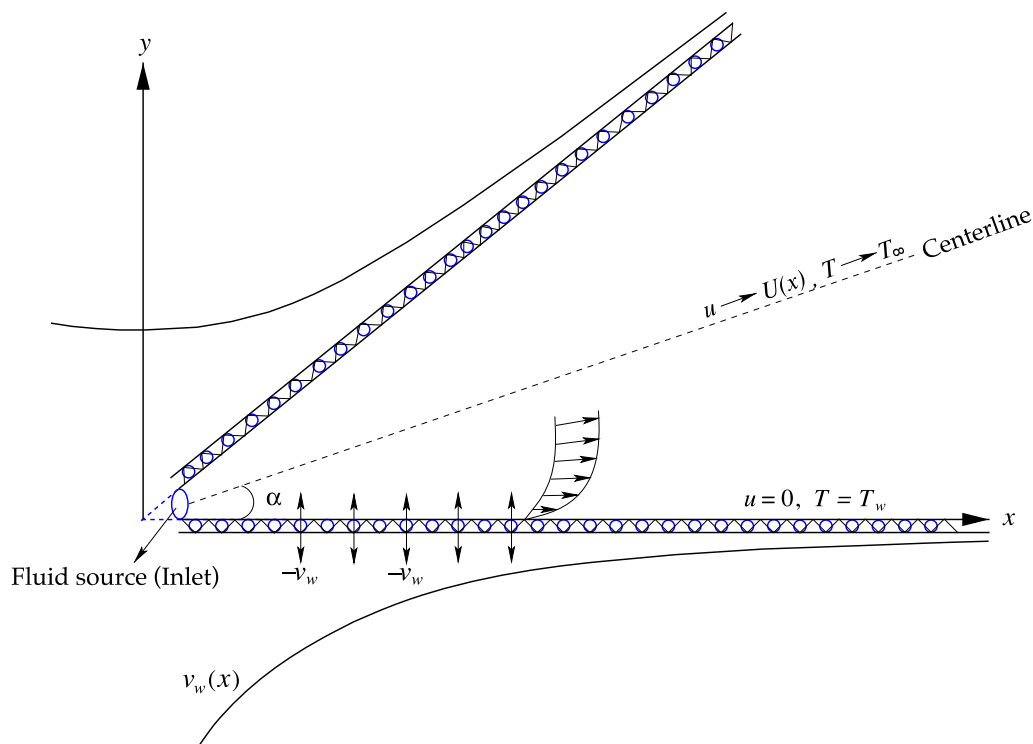


Fig. 1. A sketch of divergent channel with flow region and other details.

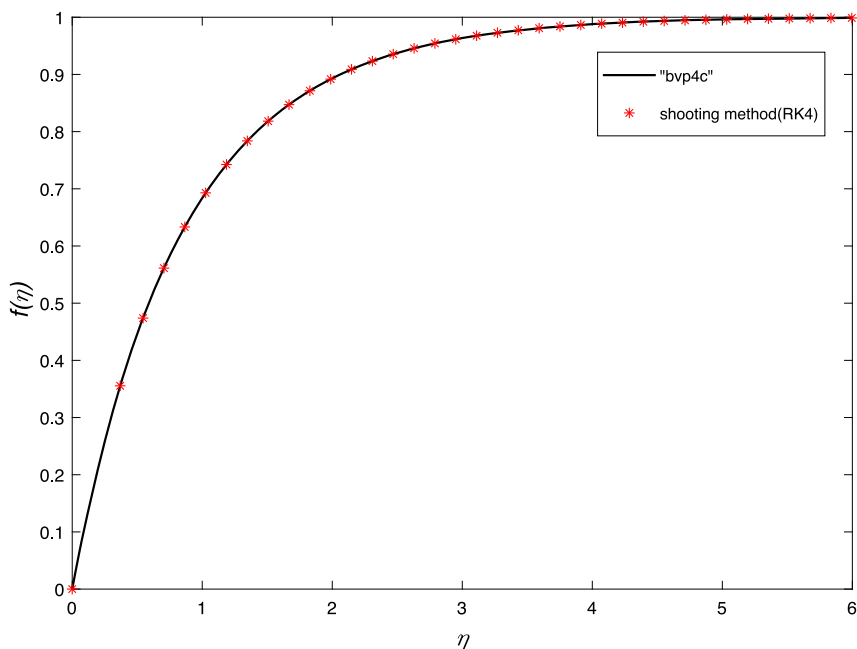


Fig. 2. Comparison of velocity profiles obtained by “bvp4c” and “shooting method with 4th order Runge-Kutta scheme” for  $\beta = 0.5$  and  $S = 5$ .

The variations in non-dimensional temperature profiles with Prandtl number( $Pr$ ) and Eckert number( $Ec$ ) are demonstrated in Figs. 7 and 8. It discloses that with rises of  $Pr$  and  $Ec$ , the temperature significantly reduces. As usual,  $Pr$  varies inversely with fluid thermal conductivity( $\kappa$ ) and it means as  $Pr$  grows,  $\kappa$  diminishes. Due to the aforesaid fact, the temperature drop is witnessed. The positive Eckert number( $Ec$ ) indicates viscous dissipation effect on the energy field. So, as  $Ec$  increases,

the impact of viscous dissipation is more prominent on the temperature profile and it causes the reduction of temperature.

The non-dimensional temperature profiles go beyond the zero level in certain situations. It means that the temperature in portion of boundary layer becomes less than the free stream temperature and the rheological characters of Casson fluid and viscous dissipation effect are the main reason behind it. Also, with increment of Prandtl number( $Pr$ )

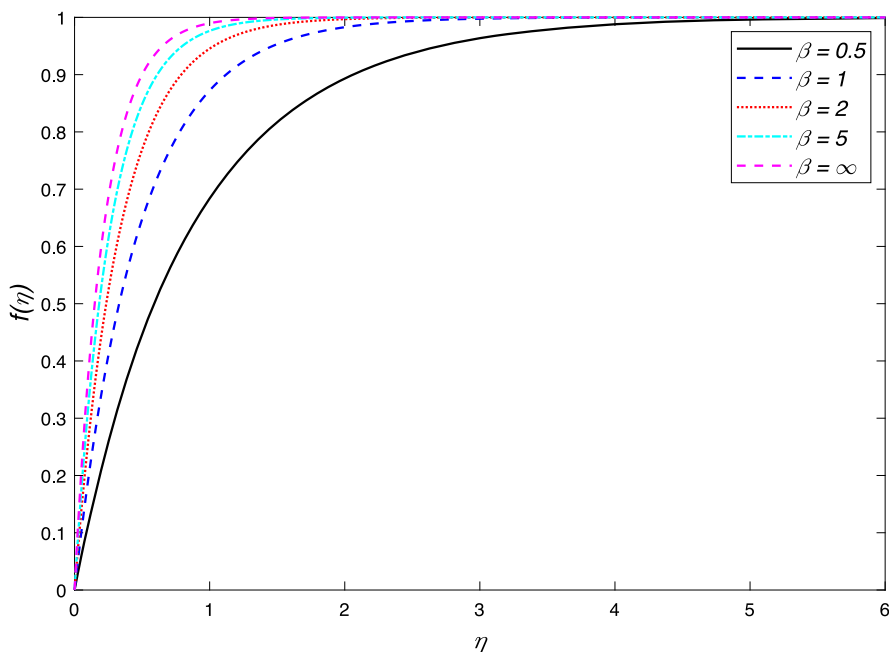


Fig. 3. Velocity  $f(\eta)$  for several  $\beta$  with  $S = 5$ .

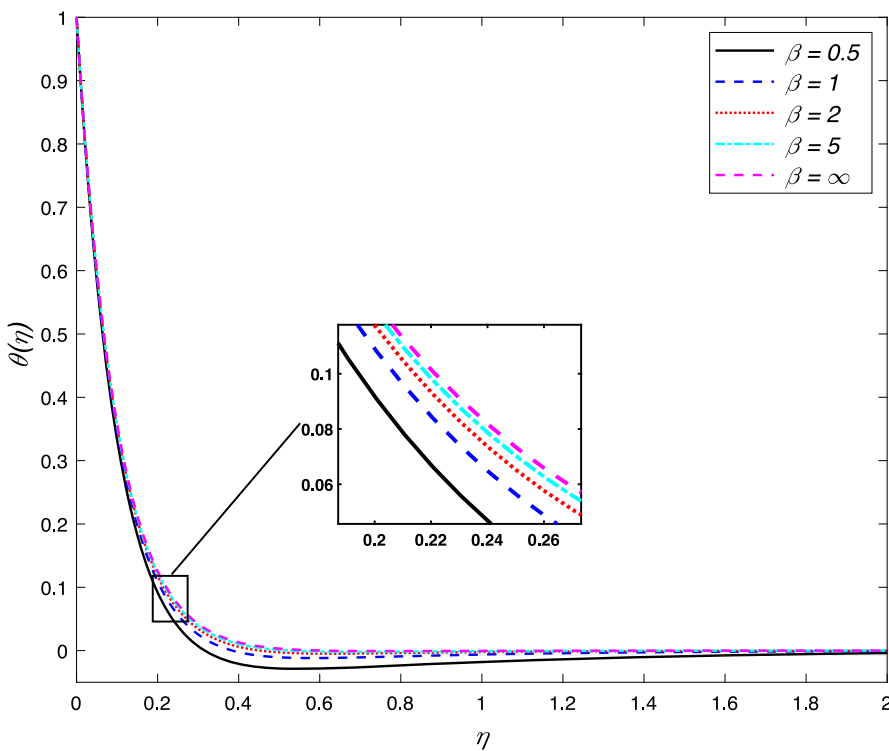


Fig. 4. Temperature  $\theta(\eta)$  for several  $\beta$  with  $S = 5$ ,  $Pr = 2$  and  $Ec = 0.1$ .

the impact of second phenomenon intensifies. This is an interesting point in boundary layer divergent channel flow.

**7. Final remarks**

From the above study of flow and heat transfer of Casson fluid in a divergent channel with suction/blowing and viscous dissipation effect the following important remarks can be summarized:

(a) Adequate amount of mass suction is necessary for existence of boundary layer flow of Casson fluid.

- (b) As Casson parameter( $\beta$ ) increases, minimum requirement of mass suction for possible boundary layer flow reduces. It means that in view of existence of boundary layer flow without separation, the better situation appears for Casson fluid flow in divergent channel when Casson parameter( $\beta$ ) is of higher level.
- (c) Increment in Casson parameter( $\beta$ ) produces augmentations of velocity and temperature. While the momentum boundary layer shrinks with  $\beta$ .
- (d) For stronger mass suction( $S > 0$ ), the momentum boundary layer thickness decreases.

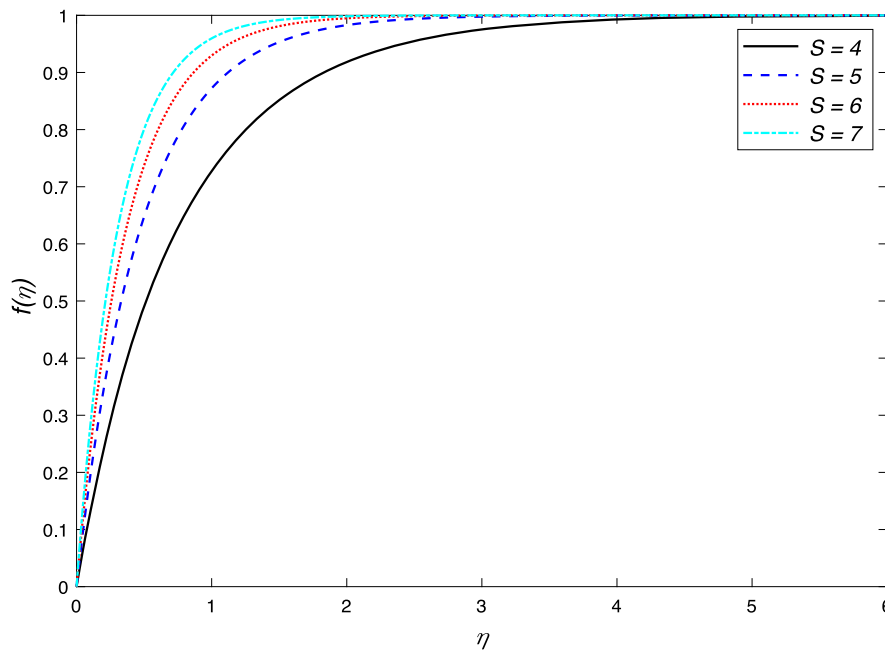


Fig. 5. Velocity  $f(\eta)$  for several  $S$  with  $\beta = 1$ .

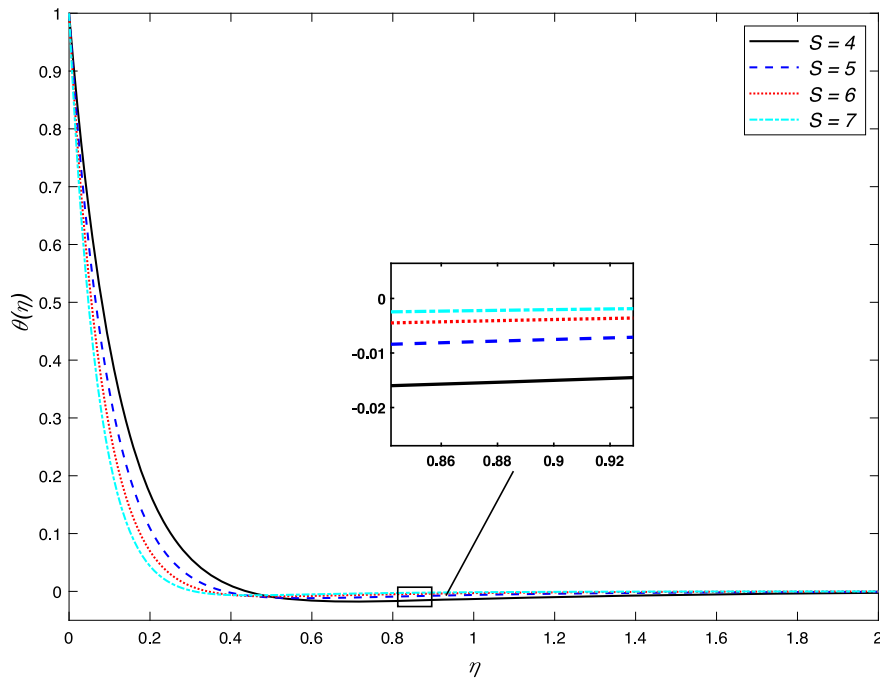


Fig. 6. Temperature  $\theta(\eta)$  for several  $S$  with  $\beta = 1$ ,  $Pr = 2$  and  $Ec = 0.1$ .

- (e) Effects of mass suction on temperature profile, near channel walls and away from the walls are opposite to each other. It firstly declines for small  $\eta$  and for large  $\eta$  it enhances.
- (f) Decay of temperature is found with Prandtl number( $Pr$ ) and Eckert number( $Ec$ ).
- (g) Due to rheological characters of Casson fluid and viscous dissipation effect temperature in some points in boundary layer drops below the level of the free stream temperature.

**Declaration of competing interest**

The authors declare that they have no known competing financial interests or personal relationships that could have appeared to influence the work reported in this paper.

**Acknowledgements**

Authors are thankful to the anonymous referees for their valuable reviews and great comments.

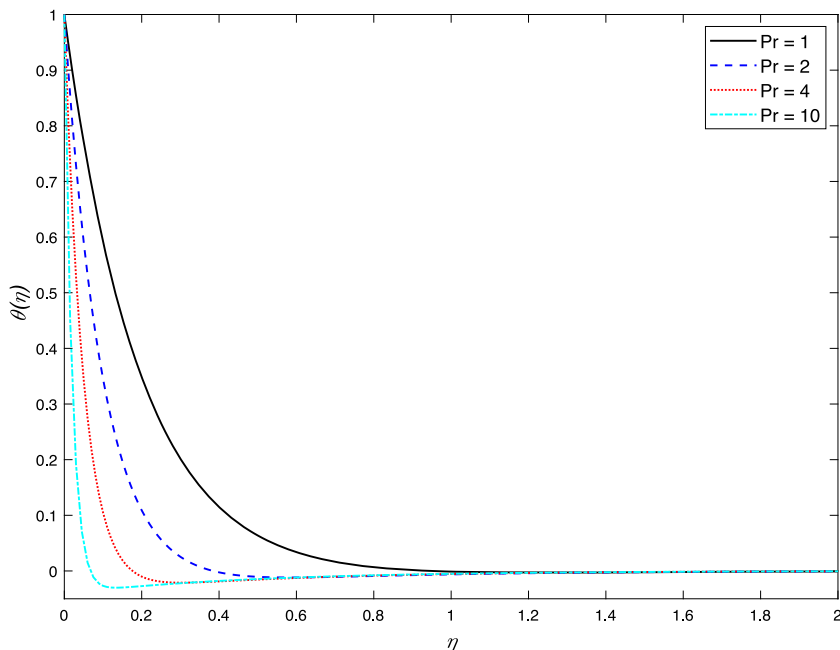


Fig. 7. Temperature  $\theta(\eta)$  for several  $Pr$  with  $\beta = 1$ ,  $S = 5$  and  $Ec = 0.1$ .

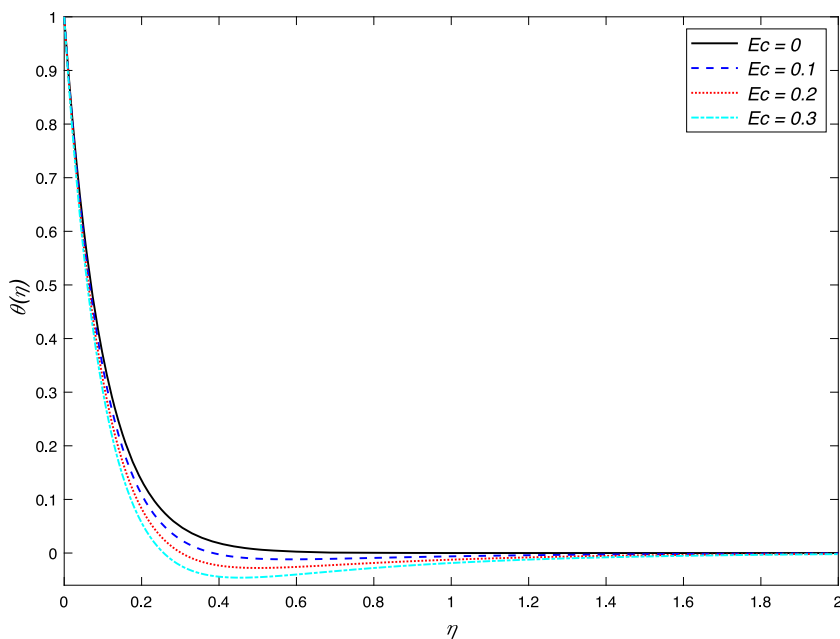


Fig. 8. Temperature  $\theta(\eta)$  for several  $Ec$  with  $\beta = 1$ ,  $S = 5$  and  $Pr = 2$ .

References

1. Jeffery GB. The two-dimensional steady motion of a viscous fluid. *Phil Mag* (6). 1915;29:455–465.
2. Hamal G. Spiralförmige bewegung zäher flüssigkeiten. *Jahresber Math-Ver.* 1916;25:34–60.
3. Pohlhausen K. Zur näherungsweise integration der differentialgleichung der laminaren grenzschrift. *ZAMM Z Angew Math Mech.* 1921;1(4):252–290.
4. Dean WR. Note on the divergent flow of fluid. *Phil Mag* (7). 1934;18:759–777.
5. Fraenkel LE. Laminar flow in symmetrical channels with slightly curved walls, I. On the Jeffery–Hamel solutions for flow between plane walls. *Proc R Soc A.* 1962;267:119–138.
6. Fraenkel LE. Laminar flow in symmetrical channels with slightly curved walls II. An asymptotic series for the stream function. *Proc R Soc A.* 1963;272:406–428.
7. Wang JW, Price GM. Laminar flow development and heat transfer in converging plane-walled channels. *Appl Sci Res.* 1972;25:361–371.
8. Ghoneim H. On the converging flow of generalized Newtonian fluid. *J Non-Newton Fluid Mech.* 1984;15:375–381.
9. Bariş S. Flow of a second-grade visco-elastic fluid in a porous converging channel. *Turk J Eng Environ Sci.* 2003;27:73–81.
10. Magyari E. Backward boundary layer heat transfer in a converging channel. *Fluid Dyn Res.* 2007;39(6):493–504.
11. Yousefi-Lafouraki B, Ramiar A, Mohsenian S. Entropy generation analysis of a confined slot impinging jet in a converging channel for a shear thinning nanofluid. *Appl Therm Eng.* 2016;105:675–685.
12. Maranzoni A, Pilotti M, Tomirotti M. Experimental and numerical analysis of side weir flows in a converging channel. *J Hydraul Eng.* 2017;143(7):04017009.
13. Holstein H. *Ähnliche Laminare Reibungsschichten an Durchlässigen Wänden*, Vol. 3050. ZWB-VM; 1943.
14. Gersten K, Körner H. Wärmeübergang unter Berücksichtigung der Reibungswärme bei laminaren Keilströmungen mit veränderlicher Temperatur und Normalgeschwindigkeit entlang der Wand. *Int J Heat Mass Transfer.* 1968;11:655–673.

15. Eagles PM. The stability of a family of Jeffery–Hamel solutions for divergent channel flow. *J Fluid Mech.* 1966;24:191–207.
16. Kamel MT. Flow of a micropolar fluid in a diverging channel. *Internat J Engrg Sci.* 1987;25:759–768.
17. Dennis SCR, Banks WHH, Drazin PG, Zaturka MB. Flow along a diverging channel. *J Fluid Mech.* 1997;336:183–202.
18. Drazin PG. Flow through a diverging channel: instability and bifurcation. *Fluid Dyn Res.* 1999;24:321–327.
19. Sadeghy K, Khabazi N, Taghavi SM. Magneto hydrodynamic (MHD) flows of viscoelastic fluids in converging/diverging channels. *Internat J Engrg Sci.* 2007;45:923–938.
20. Akulenko LD, Kumakshv SA. Bifurcation of multimode flows of a viscous fluid in a plane diverging channel. *J Appl Math Mech.* 2008;72:296–302.
21. Esmailpour M, Ganji DD. Solution of the Jeffery–Hamel flow problem by optimal homotopy asymptotic method. *Comput Math Appl.* 2010;59:3405–3411.
22. Haines PE, Hewitt RE, Hazel AL. The Jeffery–Hamel similarity solution and its relation to flow in a diverging channel. *J Fluid Mech.* 2011;687:404–430.
23. Bhattacharyya K, Layek GC. MHD boundary layer flow of dilatant fluid in a divergent channel with suction or blowing. *Chin Phys Lett.* 2011;28:084705.
24. Sheikholeslami M, Ganji DD, Ashorynejad HR, Rokni HB. Analytical investigation of Jeffery–Hamel flow with high magnetic field and nanoparticle by Adomian decomposition method. *Appl Math Mech.* 2012;33(1):25–36.
25. Layek GC, Kryzhevich SG, Gupta AS, Reza M. Steady magneto hydrodynamic flow in a diverging channel with suction or blowing. *Z Angew Math Phys.* 2013;64:123–143.
26. Gerdroodbary MB, Takami MR, Ganji DD. Investigation of thermal radiation on traditional Jeffery–Hamel flow to stretchable convergent/divergent channels. *Case Stud Therm Eng.* 2015;6:28–39.
27. Mohyud-Din ST, Khan U, Ahmed N, Hassan SM. Magneto hydrodynamic flow and heat transfer of nanofluids in stretchable convergent/divergent channels. *Appl Sci.* 2015;5:1639–1664.
28. Duryodhan VS, Singh A, Singh SG, Agrawal A. Convective heat transfer in diverging and converging microchannels. *Int J Heat Mass Transfer.* 2015;80:424–438.
29. Gepner SW, Floryan JM. Flow dynamics and enhanced mixing in a converging–diverging channel. *J Fluid Mech.* 2016;807:167–204.
30. Khan U, Adnan, Ahmed N, Mohyud-Din ST. Soret and Dufour effects on Jeffery–Hamel flow of second-grade fluid between convergent/divergent channel with stretchable walls. *Results Phys.* 2017;7:361–372.
31. Rana P, Shukla N, Gupta Y, Pop I. Analytical prediction of multiple solutions for MHD Jeffery–Hamel flow and heat transfer utilizing KKL nanofluid model. *Phys Lett A.* 2019;383(2–3):176–185.
32. Akinshilo AT, Ilegbusi A, Ali HM, Surajo A-J. Heat transfer analysis of nanofluid flow with porous medium through Jeffery Hamel diverging/converging channel. *J Appl Comput Mech.* 2020;6:433–444.
33. Liu P, Ho JY, Wong TN, Toh KC. Laminar film condensation inside and outside vertical diverging/converging small channels: A theoretical study. *Int J Heat Mass Transfer.* 2020;149:119193.
34. Fox VG, Erickson LE, Fan LT. The laminar boundary layer on a moving continuous flat sheet immersed in a non-Newtonian fluid. *AIChE J.* 1969;15:327–733.
35. Wilkinson W. The drainage of a Maxwell liquid down a vertical plate. *Chem Eng J.* 1970;1:255–257.
36. Djukic DS. Hiemms magnetic Bow of power-law fluids. *ASME J Appl Mech.* 1974;41:822–823.
37. Rajagopal KR. Viscometric flows of third grade fluids. *Mech Res Commun.* 1980;7:21–25.
38. Rajagopal KR, Gupta AS. A class of exact solutions to the equations of motion of a second grade fluid. *Internat J Engrg Sci.* 1981;19:1009–1014.
39. Rajagopal KR, Na TY, Gupta AS. Flow of a viscoelastic fluid over a stretching sheet. *Rheol Acta.* 1984;23:213–215.
40. Dorier C, Tichy J. Behavior of a Bingham-like viscous fluid in lubrication flows. *J Non-Newton Fluid Mech.* 1992;45:291–310.
41. Jafar K, Nazar R, Ishak A, Pop I. MHD mixed convection stagnation point flow of an upper convected Maxwell fluid on a vertical surface with an induced magnetic field. *Magneto hydrodynamics.* 2011;47:61–78.
42. Banerjee A, Zaib A, Bhattacharyya K, Mahato SK. MHD mixed convection flow of a non-Newtonian Powell-Eyring fluid over a permeable exponentially shrinking sheet. *Front Heat Mass Transf.* 2018;10:30.
43. Gautam AK, Verma AK, Bhattacharyya K, Banerjee A. Soret and Dufour effects on MHD boundary layer flow of non-Newtonian Carreau fluid with mixed convective heat and mass transfer over a moving vertical plate. *Pramana – J Phys.* 2020;94(1):108.
44. Verma AK, Gautam AK, Bhattacharyya K, Pop I. Entropy generation analysis in Falkner-Skan flow of Maxwell nanofluid in Darcian porous medium with temperature-dependent variable viscosity. *Pramana – J Phys.* 2021;95(2):69.
45. Ramaiah KD, Surekha P, Gangadhar K, Kannan T. MHD rotating flow of a Maxwell fluid with Arrhenius activation energy and non-Fourier heat flux model. *Heat Transf.* 2020. <http://dx.doi.org/10.1002/hjt.21717>.
46. Ramana KV, Gangadhar K, Kannan T, Chamkha AJ. Cattaneo–Christov heat flux theory on transverse MHD Oldroyd-B liquid over nonlinear stretched flow. *J Therm Anal Calorim.* 2021. <http://dx.doi.org/10.1007/s10973-021-10568-x>.
47. Casson N. A flow equation for pigment-oil suspensions of the printing ink type. In: Mill CC, ed. *Rheology of Disperse Systems*. Oxford: Pergamon Press; 1959:84–104.
48. Fredrickson AG. *Principles and Applications of Rheology*. Englewood Cliffs, N.J.: Prentice-Hall; 1964.
49. Boyd J, Buick JM, Green S. Analysis of the Casson and Carreau-Yasuda non-Newtonian blood models in steady and oscillatory flow using the lattice Boltzmann method. *Phys Fluids.* 2007;19:93–103.
50. Mustafa M, Hayat T, Pop I, Aziz A. Unsteady boundary layer flow of a Casson fluid due to an impulsively started moving flat plate. *Heat Transf Asian Res.* 2011;40:563–576.
51. Bhattacharyya K, Hayat T, Alsaedi A. Analytic solution for magneto hydrodynamic boundary layer flow of Casson fluid over a stretching/shrinking sheet with wall mass transfer. *Chin Phys B.* 2013;22:024702.
52. Bhattacharyya K, Hayat T, Alsaedi A. Exact solution for boundary layer flow of Casson fluid over a permeable stretching/shrinking sheet. *Z Angew Math Mech.* 2014;94(6):522–528.
53. Gangadhar K, Rao MVS, Ramana KV, Kumar CS, Chamkha AJ. Thermal slip flow of a three-dimensional Casson fluid embedded in a porous medium with internal heat generation. *J Nanofluids.* 2021;10:58–66.
54. Nakamura M, Sawada T. Numerical study on the flow of a non-Newtonian fluid through an axisymmetric stenosis. *ASME J Biomech Eng.* 1988;110:137–143.
55. Bhattacharyya K. Boundary layer stagnation-point flow of Casson fluid and heat transfer towards a shrinking/stretching sheet. *Front Heat Mass Transf.* 2013;4(2):023003.
56. Bhattacharyya K, Uddin MS, Layek GC. Exact solution for thermal boundary layer in Casson fluid flow over permeable shrinking sheet with variable wall temperature and thermal radiation. *Alex Eng J.* 2016;55(2):1703–1712.
57. Zaib A, Bhattacharyya\* K, Uddin MS, Shafie S. Dual solutions of non-Newtonian Casson fluid flow and heat transfer over an exponentially permeable shrinking sheet with viscous dissipation. *Model Simul Eng.* 2016;2016:6968371.
58. Gangadhar K, Kannan T, Jayalakshmi P. Magneto hydrodynamic micropolar nanofluid past a permeable stretching/shrinking sheet with Newtonian heating. *J Braz Soc Mech Sci Eng.* 2017;39:4379–4391.
59. Zaib A, Rashidi MM, Chamkha AJ, Bhattacharyya K. Numerical solution of second law analysis for MHD Casson nanofluid past a wedge with activation energy and binary chemical reaction. *Internat J Numer Methods Heat Fluid Flow.* 2017;27(12):2816–2834.
60. Gangadhar K, Keziya K, Ibrahim SM. Effect of thermal radiation on engine oil nanofluid flow over a permeable wedge under convective heating. *Multidiscip Model Mater Struct.* 2019;15:187–205.
61. Gangadhar K, Lakshmi KB, Kannan T, Chamkha AJ. Entropy generation in magnetized bioconvective nanofluid flow along a vertical cylinder with gyrotactic microorganisms. *J Nanofluids.* 2020;9:302–312.
62. Gangadhar K, Kolipaula VR, Rao MVS, Penki S, Chamkha AJ. Internal heat generation on bioconvection of an MHD nanofluid flow due to gyrotactic microorganisms. *Eur Phys J Plus.* 2020;135:600.
63. Pandey AK, Rajput S, Bhattacharyya K, Sibanda P. Impact of metal-oxide nanoparticles on unsteady stagnation-point flow of hybrid base fluid along a flat surface. *Pramana – J Phys.* 2021;95(1):5.
64. Gangadhar K, Nayak RE, Rao MVS, Kannan T. Nodal/saddle stagnation point slip flow of an aqueous convective magnesium oxide–gold hybrid nanofluid with viscous dissipation. *Arab J Sci Eng.* 2021;46:2701–2710.
65. Rao MVS, Gangadhar K, Chamkha AJ, Surekha P. Bioconvection in a convective nanofluid flow containing gyrotactic microorganisms over an isothermal vertical cone embedded in a porous surface with chemical reactive species. *Arab J Sci Eng.* 2021;46:2493–2503.
66. Banerjee A, Bhattacharyya K, Mahato SK, Chamkha AJ. Influence of various shapes of nanoparticles on unsteady stagnation-point flow of Cu-H<sub>2</sub>O nanofluid on a flat surface in porous medium: A stability analysis. *Chin Phys B.* 2021. <http://dx.doi.org/10.1088/1674-1056/ac229b>, Accepted.
67. Gangadhar K, Kannan T, Sakthivel G, Ramaiah KD. Unsteady free convective boundary layer flow of a nanofluid past a stretching surface using a spectral relaxation method. *Int J Ambient Energy* <http://dx.doi.org/10.1080/01430750.2018.1472648>.